

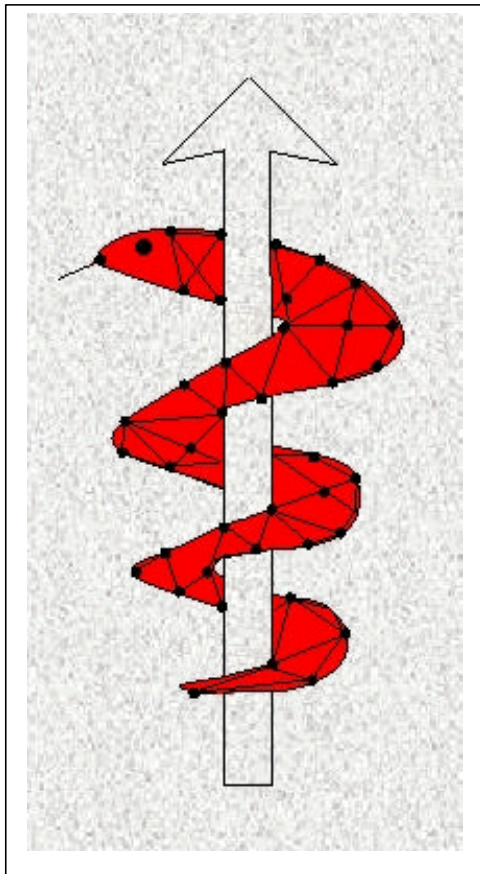


The IST Programme Project No. 10378

SimBio

SimBio - A Generic Environment for Bio-numerical Simulation

<http://www.simbio.de>



Deliverable D4.2a Inverse Field Reconstruction Design Report

Status: Final
Version: 1.1
Security: Public

Responsible: MPI
Authoring Partners: MPI

Release History

Version	Date	
0.1	15.09.00	Initial Draft
0.2	19.09.00	Pre-Release
1.0	21.09.00	Release
1.1	23.10.00	Post Review Revision

The SimBio Consortium :

NEC Europe Ltd. – UK
A.N.T. Software – The Netherlands
K.U. Leuven R&D – Belgium
ESI Group – France
Smith & Nephew - UK

MPI of Cognitive Neuroscience – Germany
Biomagnetisches Zentrum Jena – Germany
CNRS-DR18 – France
Sheffield University – UK

INVERSE FIELD RECONSTRUCTION — THE BIO-MECHANICAL TASK

ABSTRACT. The objective of modeling processes in biological tissue is twofold. On the one hand one can use such a model in order to make predictions on the properties of biological systems, the so-called forward problem like e.g. the mechanical tissue displacements induced by tumor growth. On the other hand, one can use this model in a so-called *inverse* manner to interpret measurements in terms of underlying sources. In this Workpackage, a software tool-box will be created containing inverse algorithms alongside those that are especially tailored to the validated applications from Workpackage 7. However, as we desire a modular design of the software and universality of the approaches we will provide a general tool for inverse problem solutions, but those will be tested and validated for bio-mechanical problems subject to the human brain, solely.

CONTENTS

1. Introduction	1
2. Definitions	2
3. Planned Implementation	2
3.1. Computation of deformation maps	2
3.2. Computation of probability laws	3
3.3. Inference testing on anomaly	3
3.4. Towards real time simulation	3
3.5. Interaction with other Workpackages	3
4. Current state — towards a consistent linear-elastic image registration	3
4.1. The registration algorithm	4
4.2. Alternative similarity cost functions	6
4.3. Limitations using diffeomorphisms	6
4.4. Planned extensions	7
5. Development Plan	7
References	8

1. INTRODUCTION

As there is no prior information on the underlying forces of pathological processes in the brain available, MRI time series examinations are to be employed and analyzed for non-linear vector-field transformations. This deformation fields are used to derive a force field, based on incorporated realistic material parameters. In a first approach mathematical techniques are applied for registering anatomical modalities via vector-field transformations applied to the underlying coordinate system of an anatomical template which maps template images to target images. The transformations are constraint to be consistent with the physical properties of deformable elastic solids. With this approach we may rely on the extensive work which has been emerged in the area of registration of medical images and image volumes over the last decade. Some of this work has focussed on affine transformations which account for global translation, rotation, scale and skew, while others are based on minimizing some quadratic energy penalty. Image registration algorithms use landmarks [2, 17, 22], contours [11, 25], surfaces [26], volumes [8, 25], or a combination of these features [9] to define correspondence between two images. Recently, some studies also address the topological issues involved with small- and large-distance, non-linear,

Key words and phrases. brain, bio-mechanics, deformation analysis, Finite Element Method (FEM).

volume transformations [10] and thus put explicit constraints on the bio-mechanical plausibility of such vector field transformations [see, 6, and references given there]. We will focus on this direction.

2. DEFINITIONS

In general we aim to study mathematical methods in the framework of the emerging discipline of *Computational Anatomy*. Herein MPI will basically follow the *Grenander model* of anatomy¹ introduced in [14], in which anatomies are represented as deformable templates, in our case as collections of 3-dimensional manifolds. Typical structure is carried by the template via the application of transformations to the background manifolds. The anatomical model is a quadruple $(\Omega, \mathcal{H}, \mathcal{I}, \mathcal{P})$: with background space Ω , the set of transformations on the background space $\mathcal{H} : \Omega \leftrightarrow \Omega$, the space of idealized medical imagery \mathcal{I} , and the family of probabilistic measures on \mathcal{H} .

There are three principle components to computational anatomy we study in subtask 4.2:

1. *Computation of deformation maps*: Given any two elements $I_n, I_m \in \mathcal{I}$ in the same space $(\Omega, \mathcal{H}, \mathcal{I})$, compute diffeomorphisms² h with inverses h^{-1} from one anatomy to the other $I_n \xrightleftharpoons[h_n^{-1}]{h_n m} I_m$. This is the principle method by which anatomical structures are understood, transferring the emphasis from the image $I \in \mathcal{I}$ to the structural transformations that generate them, and the basis for our bio-mechanical inversion task.
2. *Computation of probability laws*: Given populations of anatomical imagery and diffeomorphisms between them $I_n \xrightleftharpoons[h_n^{-1}]{h_n m} I_m, n, m = 1, \dots, N \subset \mathcal{H}$ generate probability laws $P \in \mathcal{P}$ on \mathcal{H} which represent anatomical variation reflected by the observed population of transformations h [cf., 14, 20].
3. *Inference and testing on anomalies*: Within the anatomy $(\Omega, \mathcal{H}, \mathcal{I}, \mathcal{P})$, perform a classification and testing for anomalies, eventually singularities, for pathological processes.

3. PLANED IMPLEMENTATION

3.1. Computation of deformation maps. Instead of pixel-based approaches we prefer to base the analysis on the Euclidean space in which the brain structures actually reside. In this approach, the maps are used to analytically compute classical formulas from differential geometry on transformations on tangent spaces in the brain under the Jacobian and Hessian. For this the transformations must be established on a continuum. Variability of the images (and FE meshes later) is studied through the transformations $h \in \mathcal{H}$:

$$h : x \doteq (x_1, x_2, x_3) \in \Omega \mapsto h(x) \doteq \underbrace{(h_1(x), h_2(x), h_3(x))}_{\doteq x + u(x)} \in \Omega,$$

where we will study the transformations in terms of the so-called Eulerian displacement $u(\cdot)$. The positive sign gives the interpretation of flow; a particle at position x originated at point $x + u(x)$ in the original coordinate system.

¹which is based upon global pattern theory introduced by [12, 13]

²as a first approach we assume all transformations to be diffeomorphic, i.e. continuous, 1-to-1, onto and differentiable [21].

3.2. Computation of probability laws. The Bayesian approach to understand complex brain variability is to construct several templates containing the topological structures of complex anatomy. Upon this a probability measure is constructed on the space of \mathbb{R}^3 valued vector field transformations \mathcal{H} . This is the representation of biological variability. The prior measure encodes probabilistic properties of the map that are required for understanding the various differential geometric invariants and physical features such as distance, surfaces and volumes in the family of possible anatomies. The template and the prior measure specify the global anatomical relationships between structures as well as how they can vary from one brain to another. Formulations of statistical methods focusing on computational anatomy are presented by [20].

3.3. Inference testing on anomaly. Based on registration, we will extract displacement fields and detect force fields. In a next step, these data can be analyzed for normal biological variability as well as for pathological processes. In doing so, the respective vector fields might need to be simplified first by finding critical points like attractors, repellers and saddle points, which are immanent to the field. Anatomical landmarks may serve as a coordinate system basis to describe the position of these critical points. The resulting map of internal forces can be passed to the mesh generation for further exploration and forward simulation on the initial MRI data.

By testing anomalies corresponding to pathological processes we will focus on the inversion of internal forces subject to focal brain damage and neuro-degenerative diseases.

3.4. Towards real time simulation. As the software from this project sub-task is supposed to become a supportive tool for clinicians (see TA) we have to aim for real-time simulations. For the bio-mechanical application this implies, for instance, that the SimBio environment permits the clinician to virtually operate on the real patient's scanned and meshed body part of interest, which he sees on the screen. Beyond the capability of the visualization tool (see report Workpackage 5) to deliver high upgrade rates of the simulation results this implies that special attention within this project task has to be dedicated to performance tests to gain highest efficiency.

3.5. Interaction with other Workpackages. With regard to the applications in Workpackage 7, the algorithms will be tailored to deduce displacements and reconstruct sources of mechanical forces from time series measurements by plausible bio-mechanical models.

Within the progress of the project we will adapt methods developed for image registration to FE meshes with the aim of performing elastic registrations on those. Herein we depend on the work done in Workpackages 1 (Segmentation/Mesh generation) and 2 (Material database) to have segmented imagery and to gain vantage from robust knowledge about tissue elasticity. We further plan to exploit the inversion solutions to simple forward simulations on the initial MRI data (see 3.3). Herein we rely on Workpackage 2. Beyond the development task our focus will lie on the modularity of the software as to its performance. Regarding the latter there might appear the necessity to participate from the solver techniques developed in Workpackage 3.

4. CURRENT STATE — TOWARDS A CONSISTENT LINEAR-ELASTIC IMAGE REGISTRATION

A fundamental problem with a large class of image registrations techniques is that the estimated transformation from one image T to another image S does not equal the inverse of the estimated transform from S to T . This inconsistency is a result of the matching criteria's inability to uniquely describe the correspondences between two images. MPI will follow an algorithm introduced by [6] which seeks to overcome this limitation by jointly investigating the transformations h from T to S and g from S to T (see Fig. 4) while enforcing the consistency constraint that these transformations are inverse to one another³.

³Ideally, the transformations h and g should be uniquely determined and should be inverse of one another. However, estimating h and g independently very rarely results in a consistent set of transformations due to a large

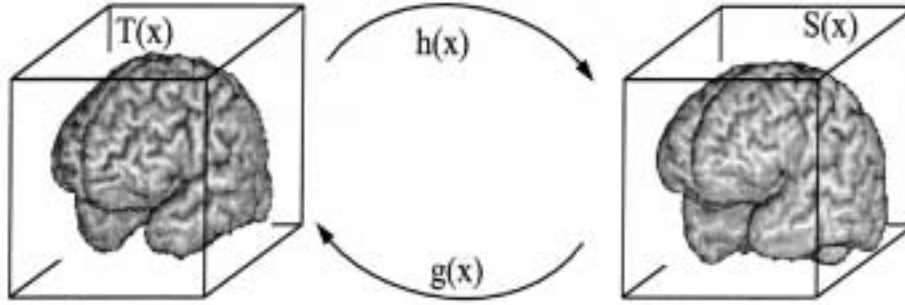


FIGURE 1. Consistent image registration is based on the principle that mappings h from T to S and g from S to T define a point by point correspondence between T and S that are consistent with each other. This consistency is enforced mathematically by jointly estimating h and g while constraining h and g to be inverse mapping to another (this figure is courtesy of *G. Christensen*, [cf., 6])

The transformations are further restricted to preserve topology by constraining them to obey the laws of continuum mechanics. The transformations are parametrized by a Fourier series to diagonalize the covariance structure [20] imposed by the continuum mechanics constraints [7] and to provide a computationally efficient numerical implementation. In a first step MPI will (a) adapt the method for MRI using linear elastic material constraints and (b) restrict the class of applications that can be solved using diffeomorphic transformations (see 4.3 for limitations of this approach). Diffeomorphic transformations maintain the topology p.d. [15, 16] and guarantee that connected subregions of an image remain connected, neighborhood relationships between structures are preserved, and surfaces are mapped to surfaces.

4.1. The registration algorithm. The registration problem can be stated as:

Problem 4.1. Jointly estimate the transformations h and g such that h maps T to S and g maps S to T subject to the constraint that $h = g^{-1}$.

We assume that the 3D image volumes T and S are MRI images collected from similar anatomical populations. Each image is defined to be a function of $x \in \Omega = [0, 1]^3$. The transformations are vector-valued functions that map the image domain Ω to itself, i.e., $h : \Omega \mapsto \Omega$ and $g : \Omega \mapsto \Omega$. Diffeomorphic constraints are placed on h and g so that they preserve topology. Throughout it is assumed that $h(x) = x + u(x)$, $h^{-1}(x) = x + \tilde{u}(x)$, $g(x) = x + w(x)$ and $g^{-1}(x) = x + \tilde{w}(x)$, where $h(h^{-1}(x)) = x$ and $g(g^{-1}(x)) = x$. All fields h, g, u, \tilde{u}, w and $\tilde{w}(x)$ are (3×3) vector-valued functions of $x \in \Omega \mapsto \Omega$. Registration is defined by using a symmetric cost function $C(h, g)$ that describes the distance between the transformed template $T(h)$ and target S , and the distance between the transformed target $S(g)$ and template T . To ensure the desired properties, the transformations h (forward transformation) and g (reverse transformation) are jointly estimated by minimizing the cost function $C(h, g)$ while satisfying diffeomorphic constraints and inverse consistency constraints. The diffeomorphic constraints are enforced on the transformations by constraining them to satisfy the laws of continuum mechanics [23].

To overcome correspondence ambiguities, the transformations from T to S and from S to T are jointly estimated. The transformations h and g are estimated by minimizing a cost function that is a function of $(T(h(x)) - S(x))$ and $(S(g(x)) - T(x))$. Following [6] we initially (cf. 4.2) use a cost function based on image intensity:

number of local minima. The inverse consistency constraint reduces the number of local minima because the problem is solved from two different directions.

$$C_1(T(h), S) + C_1(S(g), T) = \int_{\Omega} |T(h(x)) - S(x)|^2 dx + \int_{\Omega} |S(g(x)) - T(x)|^2 dx.$$

This cost function does guarantee that h and g are inverse of each other, because the respective contributions of h and g to the cost functions are independent. In order to couple the estimation of h and with that of g , [6] we impose an additional inverse transformation consistency constraint that is minimized when $h = g^{-1}$:

$$\begin{aligned} C_2(u, \tilde{w}) + C_2(w, \tilde{u}) &= \int_{\Omega} \|u(x) - \tilde{w}(x)\|^2 dx + \int_{\Omega} \|w(x) - \tilde{u}(x)\|^2 dx \\ &= \int_{\Omega} \|h(x) - g^{-1}(x)\|^2 dx + \int_{\Omega} \|g(x) - h^{-1}(x)\|^2 dx, \end{aligned}$$

where $h(x) = x + u(x)$, $h^{-1}(x) = x + \tilde{u}(x)$, $g(x) = x + w(x)$, $g^{-1}(x) = x + \tilde{w}(x)$. The inverse transformation h^{-1} is computed from h by solving the minimization problem $h^{-1}(y) = \arg \min_x \|y - h(x)\|^2$ for each y on a discrete lattice in Ω . The inverse of the reverse transformation g^{-1} is computed from w similarly. A sufficient condition to ensure that the inverse transformation h^{-1} exists and is unique is that h is a diffeomorphism. However, minimizing C_2 does not ensure that the transformations h and g are diffeomorphic transformations except when $C_2(h, g) = 0$. To enforce the transformations to be diffeomorphic a continuum mechanical model is applicable such as linear elasticity [4, 9] or viscous fluid [5, 8, 9]. Thus, a cost function of the form

$$C_3(u) + C_3(w) = \int_{\Omega} \|\mathcal{L}u(x)\|^2 dx + \int_{\Omega} \|\mathcal{L}w(x)\|^2 dx$$

can be used to enforce the diffeomorphic property. In a first approach we follow here [6] and choose the operator \mathcal{L} to describe linear-elasticity:

$$\begin{aligned} \mathcal{L} &= -\alpha\Delta - \beta\nabla\nabla + \gamma I \\ &= \begin{pmatrix} -\alpha\Delta - \beta\frac{\partial^2}{\partial x_1^2} + \gamma & -\beta\frac{\partial^2}{\partial x_1\partial x_2} & -\beta\frac{\partial^2}{\partial x_1\partial x_3} \\ -\beta\frac{\partial^2}{\partial x_2\partial x_1} & -\alpha\Delta - \beta\frac{\partial^2}{\partial x_2^2} + \gamma & -\beta\frac{\partial^2}{\partial x_2\partial x_3} \\ -\beta\frac{\partial^2}{\partial x_3\partial x_1} & -\beta\frac{\partial^2}{\partial x_3\partial x_2} & -\alpha\Delta - \beta\frac{\partial^2}{\partial x_3^2} + \gamma \end{pmatrix}, \end{aligned}$$

but in general \mathcal{L} can be any non-singular linear differential operator (or any other non-singular differential operator that can be linearized)[20]⁴.

To parameterize the forward and reverse transformations a 3D Fourier series representation is used. As the Fourier series parameterization is periodic in x each basis coefficient can be interpreted as the weight of a harmonic component in a single coordinate direction. The displacement fields have the form:

$$u(x) = \sum_{i=0}^{N_1-1} \sum_{j=0}^{N_2-1} \sum_{k=0}^{N_3-1} \mu_{ijk} e^{j\langle x, \omega_{ijk} \rangle} \quad \text{and} \quad w(x) = \sum_{i=0}^{N_1-1} \sum_{j=0}^{N_2-1} \sum_{k=0}^{N_3-1} \eta_{ijk} e^{j\langle x, \omega_{ijk} \rangle},$$

where μ_{ijk} and η_{ijk} , the basis coefficients, are 3×1 , complex-valued vectors and $\omega \doteq [2\pi i/N_1, 2\pi j/N_2, 2\pi k/N_3]$. It is assumed that the images T and S are represented as $N_1 \times N_2 \times N_3$ voxel volumes. The coefficients μ_{ijk} and η_{ijk} are constrained to have complex conjugate symmetry during the estimation process.

Such Fourier series parameterization is a multi-resolution decomposition of the displacement fields. In practice, the low frequency basis coefficients are estimated before

⁴as long as the 3×3 matrix Green's function is continuous.

the higher allowing the global image features being registered before the local features. This is accomplished by replacing the above displacement representations by

$$u(x) = \sum_{i=-d_1}^{d_1} \sum_{j=-d_2}^{d_2} \sum_{k=-d_3}^{d_3} \mu_{ijk} e^{j\langle x, \omega_{ijk} \rangle} \quad \text{and} \quad w(x) = \sum_{i=-d_1}^{d_1} \sum_{j=-d_2}^{d_2} \sum_{k=-d_3}^{d_3} \eta_{ijk} e^{j\langle x, \omega_{ijk} \rangle}.$$

The values of d_1 , d_2 , and d_3 are initially set small and are periodically increased throughout the iterative minimization procedure. The constants d_1 , d_2 , and d_3 represent the largest x_1 , x_2 , and x_3 harmonic components of the displacement fields, respectively. Such representation can be computed efficiently using 3D FFT's.

The registration problem can now be restated by combining the above Eqs. for C_1 , C_2 , and C_3 and estimating the set of parameters $\{\hat{\mu}_{ijk}, \hat{\eta}_{ijk}\}$ that minimize the cost function

$$\begin{aligned} \hat{h}(x), \hat{g}(x) = \arg \min_{h(x), g(x)} & \int_{\Omega} |T(h(x)) - S(x)|^2 + |S(g(x)) - T(x)|^2 dx \\ & + \lambda \int_{\Omega} \|u(x) - \tilde{w}(x)\|^2 + \|w(x) - \tilde{u}(x)\|^2 dx \\ & + \rho \int_{\Omega} \|\mathcal{L}u(x)\|^2 + \|\mathcal{L}w(x)\|^2 dx \end{aligned}$$

where the constants λ and ρ are Lagrange multipliers to enforce/balance the constraints [6]. In a first approach, the transformations \hat{h} and \hat{g} are estimated by using a gradient decent algorithm to detect the basis coefficients $\{\mu_{ijk}, \eta_{ijk}\}$. The respective gradient decent equations are given by [7]. As it turns out those equations can partly be combined and computed efficiently using 3D FFT's which significantly improves the performance of the algorithm.

4.2. Alternative similarity cost functions. The demons [3, 25] algorithm may be used. Alternatively, other cost functions may be used such as the mutual information cost function [19] to define correspondences. The mutual information cost function has the advantage of being able to specify the correspondence between images collected from the same or different image modalities, can be formulated on a basis other than intensity and is thus probably more likely to be applicable for FE-mesh registrations.

There are many other similarity cost functions that use features such as e.g., gradient magnitude, landmarks and edges. All of these features can be used to define similarity cost functions. For instance, a symmetric cost function based on the gradient magnitude of an image could have the form:

$$C'_1 = \int_{\Omega} (\|\nabla T(h(x))\| - \|\nabla S(x)\|)^2 dx + \int_{\Omega} (\|\nabla S(g(x))\| - \|\nabla T(x)\|)^2 dx.$$

4.3. Limitations using diffeomorphisms. Diffeomorphic transformations are not necessarily valid for registering images collected from the same individual before and after surgery. A diffeomorphic mapping assumption may be valid for registering MRI data from two different normal individuals if the goal is to match the deep nuclei of the brain, but it may not be valid for the same data set if the task is to match the sulcal patterns.

Alternatively, diffeomorphic transformations may be used to identify areas where two image volumes differ topologically by analyzing the properties of the resulting transformations. For instance, if matching an MRI image with a tumor to one without a tumor, a valid diffeomorphic transformation may be one that registers all of the corresponding brain structures by shrinking the tumor to a small point. Such a transformation would have an unusually small Jacobian which could be used to detect or identify the location of the tumor. Conversely, for the inverse problem of matching the image without the tumor to one

with a tumor, a valid registration is to register all of the corresponding brain structures by allowing the transformation to tear (i.e., not diffeomorphic) at the site of the tumor [20].

4.4. Planned extensions. As stated above, MPI has implemented a gradient decent approach for the minimization task of the cost function. This will certainly be replaced by more sophisticated optimizations algorithms such as momentum term support [1] or conjugate gradient [24] methods to achieve a more stable and faster convergence.

The elasticity operator \mathcal{L} used within C_2 yet only accounts for linear elasticity. Within the progress of the project we will extent the method to non-linear (e.g., viscous fluid) elastic transformations and (depending on the work done in Workpackages 1 and 2) to handle segmented images, and thus being applicable to FE meshes, in order to achieve a better performance (less nodes than image pixels) and to gain vantage from robust knowledge about tissue elasticity.

Much like [7], we assume that a valid transformation is diffeomorphic everywhere except possibly in regions where the source and the target image differ topologically, e.g., in the neighborhood of a tumor. This idea can be extended to non-diffeomorphic mapping by including the proper boundary conditions around regions that differ topologically [for a non-linear FE formulation to that scenario see, e.g., 18]. However, the purpose of the above mentioned diffeomorphic constraint is to ensure that the transformations maintain the topology of source T and target S . Thus, the diffeomorphic constraint might also be replaced by or combined with other regularization constraints that maintains desirable properties of the template (source) and target when deformed. An example would be a constraint that prevents the Jacobian of both the forward and the reverse transformations from going to zero or infinity. A constraint of this type that penalizes small and large Jacobian values is given by:

$$C_4(h) + C_4(g) = \int_{\Omega} \left(J(h(x)) + \frac{1}{J(h(x))} \right)^2 dx + \int_{\Omega} \left(J(h(x)) + \frac{1}{J(h(x))} \right)^2 dx,$$

where J denotes the Jacobian operator⁵.

It can be shown, however, that the described method is according to the diffeomorphism assumption restricted to small deformations, only [4], but within the progress of the project it might be possible to handle even large deformations. Initial ideas to that are presented by [8, 17].

5. DEVELOPMENT PLAN

In accordance with the above described shortcomings of the 'consistent registration' method (4.3), with its extension plan (4.4) and regarding (3.3), MPI will concentrate on the following schedule (in an arbitrary order):

- improve optimization schemes
- improve performance by parallelization
- study of image similarity term
- incorporate of variable elasticity/viscosity
- sensitivity analysis
- study of modeling errors
- analyze vector fields regarding critical points
- find probability measures for the inverted vector fields that resemble biological variety
- focus on pathological processes (degenerative diseases: morbus Alzheimer, hypertensive encephalopathy; focal lesions: cerebral infarcts, hemorrhages)

⁵ $J(h(x)) = \det |\nabla h|_x$ and $J(g(x)) = \det |\nabla g|_x$, respectively.

REFERENCES

1. C. M. Bishop, *Neural networks for pattern recognition*, 2nd ed., Calderon Press, Oxford, 1995.
2. F. L. Bookstein, *Morphometric tools for landmark data*, Cambridge Univ. Press, New York, 1991.
3. P. Cachier, X. Pennec, and N. Ayache, *Fast non-rigid matching by gradient descent: study and improvements of the "demons" algorithm*, Technical Report 3706, INRIA, Sophia-Antipolis, Jun. 1999.
4. G. E. Christensen, R. D. Rabbitt, and M. I. Miller, *3D brain mapping using deformable neuroanatomy*, *Phys. Med. Biol.* **39** (1994), 609–618.
5. G. E. Christensen, *Deformable shape models for neuroanatomy*, DSc.-thesis, Server Institute of Technology, Washington University, Saint Louis, 1994.
6. ———, *Consistent linear-elastic transformations for image matching*, *Information Processing in medical imaging* (A. Kuba, M. Šámal, and A. Todd-Pokropek, eds.), *Lect. Notes Comp. Sci.*, vol. 1613, Springer-Verlag, Berlin · Heidelberg, 1999, pp. 224–237.
7. ———, *Consistent image registration*, submitted to *IEEE Trans. Med. Imag.*, 2000.
8. G. E. Christensen, R. D. Rabbitt, and M. I. Miller, *Deformable templates using large deformation kinematics*, *IEEE Trans. Medical Imag.* **5** (1996), no. 10, 1435–1447.
9. G.E. Christensen, S. C. Joshi, and M. I. Miller, *Volumetric transformations of brain anatomy*, *IEEE Trans. Medical Imag.* **16** (1997), no. 6, 864–877.
10. R. D. Christensen, G. E. ad Rabbitt, M. I. Miller, S. C. Joshi, U. Grenander, T. A. Coogan, and D. C. van Essen, *Topological properties of smooth anatomic maps*, *Information Processing in Medical Imaging* (Y. Bizais, ed.), Kluwer Academic Publisher, 1995, pp. 101–112.
11. C. A. Davatzikos, J. L. Prince, and R. N. Bryan, *Image registration based on boundary mapping*, *IEEE Trans. Medical Imag.* **15** (1996), no. 1, 112–115.
12. U. Grenander, *General pattern theory: A methematical study of regular structures*, *oxford mathematical monographs ed.*, Oxford Uni. Press, 1994.
13. ———, *Elemants of pattern theory*, *John Hopkins Series in Mathematical Science*, John Hopkins Univ. Press, 1995.
14. U. Grenander and M. I. Miller, *Computational anatomy: An emerging discipline*, *Quaterly Appl. Math.* **LVI** (1998), no. 4, 617–694.
15. K. Jänich, *Vektoranalysis (in german)*, 2nd ed., Springer-Verlag, Berlin · Heidelberg, 1993.
16. ———, *Topologie (in german)*, 9th ed., Springer-Verlag, Berlin · Heidelberg, 1999.
17. S. C. Joshi and M. I. Miller, *Landmark matching via large deformation diffeomorphisms*, *IEEE Trans. Medical Imag.* **9** (2000), no. 8, 1357–1370.
18. S. K. Kyriacou, C. Davatzikos, S. J. Zinreich, and R. N. Bryan, *Non-linear elastic registration of brain images with tumor pathology using a biomechanical model*, *IEEE Trans. Medical Imag.* **18** (1999), no. 7, 580–592.
19. F. Maes, A. Collignon, D. Vandermeulen, G. Marchal, and P. Suetens, *Multi-modal volume registration by maximization of mutual information*, *IEEE Trans. Medical Imag.* **16** (1997), no. 2, 187–198.
20. M. Miller, A. Banerjee, Christensen G., S. Joshi, N. Khaneja, U. Grenander, and L. Matejic, *Statistical methods in computational anatomy*, *Stat. Meth. Medical Res.* **6** (1997), 267–299.
21. M. Nakahara, *Geometry, Topology and Physics*, *Graduate student series in physics*, IoP, London, 1998.
22. K. Rohr, M. Fornefett, and H. S. Stiehl, *Approximating thin-plate splines for elastic registration: Itegration of landmark errors and orientation attributes*, *Information Processing in Medical Imaging* (A. Kuba, M. Šámal, and A. Todd-Pokropek, eds.), *Lect. Notes Comp. Sci.*, vol. 1613, Springer-Verlag, Berlin · Heidelberg, Jun. 1999, pp. 252–265.

23. L. A. Segel, *Mathematics applied to continuum mechanics*, Dover classics of Science and Mathematics, Dover Publ., New York, 1987.
24. J. R. Shewchuk, *An introduction to the conjugate gradient method without the agonizing pain*, Tech. Report CMU-CS-94-125, School of Computer Science, Carnegie Mellon University, Pittsburgh, March 1994.
25. J. P. Thirion, *Image matching as a diffusion process: An analogy with Maxwell's demon*, *Medical Imag. Analysis* **2** (1998), 243–260.
26. P. M. Thompson and A. W. Toga, *A surface based technique for warping three-dimensional images of the brain*, *IEEE Trans. Medical Imag.* **15** (1996), no. 4, 1–16.

DR. M. TITTEMEYER & DR. F. KRUGGEL, MPI COGNITIVE NEUROSCIENCE, STEPHANSTR.1A, 04103 LEIPZIG, GERMANY

E-mail address: {tittge,kruggel}@cns.mpg.de